

pH-dependent Binding of the Epsin ENTH Domain and the AP180 ANTH Domain to PI(4,5)P₂-containing Bilayers

Robert A. Hom¹†, Mohsin Vora²†, Maryann Regner¹
Oksana M. Subach³, Wonhwa Cho⁴, Vladislav V. Verkhusha³
Robert V. Stahelin^{2,5} and Tatiana G. Kutateladze^{1*}

¹Department of Pharmacology
University of Colorado Health
Sciences Center, Aurora
CO 80045, USA

²Department of Biochemistry
and Molecular Biology
Indiana University School of
Medicine-South Bend
South Bend, IN 46617, USA

³Department of Anatomy and
Structural Biology, Albert
Einstein College of Medicine
Bronx, New York 10461, USA

⁴Department of Chemistry
University of Illinois at Chicago
Chicago, IL 60607, USA

⁵Department of Chemistry and
Biochemistry and The Walther
Center for Cancer Research
University of Notre Dame
South Bend, IN 46617, USA

Received 16 July 2007;
received in revised form
7 August 2007;
accepted 7 August 2007
Available online
21 August 2007

Edited by M. F. Summers

Epsin and AP180 are essential components of the endocytotic machinery, which controls internalization of protein receptors and other macromolecules at the cell surface. Epsin and AP180 are recruited to the plasma membrane by their structurally and functionally related N-terminal ENTH and ANTH domains that specifically recognize PtdIns(4,5)P₂. Here, we show that membrane anchoring of the ENTH and ANTH domains is regulated by the acidic environment. Lowering the pH enhances PtdIns(4,5)P₂ affinity of the ENTH and ANTH domains reinforcing their association with lipid vesicles and monolayers. The pH dependency is due to the conserved histidine residues of the ENTH and ANTH domains, protonation of which is necessary for the strong PtdIns(4,5)P₂ recognition, as revealed by liposome binding, surface plasmon resonance, NMR, monolayer surface tension and mutagenesis experiments. The pH sensitivity of the ENTH and ANTH domains is reminiscent to the pH dependency of the FYVE domain suggesting a common regulatory mechanism of membrane anchoring by a subset of the PI-binding domains.

© 2007 Elsevier Ltd. All rights reserved.

Keywords: PtdIns(4,5)P₂; ENTH; epsin; ANTH; membrane

*Corresponding author. E-mail address: Tatiana.Kutateladze@UCHSC.edu.

† R.A.H. and M.V. contributed equally to the work.

Abbreviations used: ENTH, Epsin N-terminal homology; ANTH, AP180 N-terminal homology; GST, glutathione S-transferase; SUV, small unilamellar vesicle; SPR, surface plasmon resonance; EGFP, enhanced green fluorescent protein; HSQC, heteronuclear single quantum coherence; POPC, 1-palmitoyl-2-oleoyl-sn-glycero 3-phosphocholine; POPE, 1-palmitoyl-2-oleoyl-sn-glycero-3-phosphoethanolamine; POPS, 1-palmitoyl-2-oleoyl-sn-glycero-3-phosphoserine.

Introduction

Clathrin-mediated endocytosis is one of the major mechanisms for internalization of cell surface receptors, growth factors and other extracellular macromolecules inside the cell.^{1–3} Clathrin promotes invagination of the plasma membrane and formation of a coated pit which then buds into the cytoplasm and after fission produces a small transport vesicle containing the internalized cargo. Once endocytosed, the vesicle fuses with early endosomes and the cargo either recycles back to the plasma membrane or is forwarded to the lysosome for degradation. The initial steps of endocytosis, membrane budding and formation of vesicles require the clathrin tri-skeleton assembly stimulated by the adaptor complex AP-2 and multiple accessory co-factors.^{1,4,5} Two accessory proteins, Epsin and AP180, initiate the formation of a pit by docking to the plasma membrane and recruiting and promoting polymerization of clathrin. It has been reported that membrane association of Epsin and AP180 is primarily mediated by their amino-terminal domains that recognize PtdIns(4,5)P₂.^{4,6–11} Once bound to the lipid, Epsin modifies the membrane curvature and induces tubulation of liposome bilayers and the plasma membrane in living cells,⁸ while AP180 stimulates clathrin assembly at newly invaginated synaptic vesicles but does not deform membranes.^{6,9}

The Epsin N-terminal homology (ENTH) domain, a conserved ~150 residue module, was discovered in 1999^{12,13} and has since been identified in all members of the Epsin family (SMART). Found exclusively at the amino-termini, the ENTH domain recruits Epsin to the plasma membrane through specific, ~0.37 μM-affinity interaction with PtdIns(4,5)P₂.⁷ Cell localization studies indicate that PtdIns(4,5)P₂ recognition by the ENTH domain is sufficient for the strong membrane association. The PI binding of the ENTH domain also plays a role in membrane anchoring of clathrin, AP-2, Eps15 and intersectin as these components of endocytotic machinery bind a long unstructured sequence following the ENTH domain in the majority of Epsin proteins.^{12,14–16} Mutations in the ENTH domain that abolish lipid binding or truncation of the entire domain have a dominant negative effect on endocytosis of epidermal growth factor, likely due to the loss of the ability to recruit the endocytotic assembly to the plasma membrane.^{7,8,10}

The ENTH domain folds in a compact structure consisting of eight α-helices packed in three twisted helical hairpins.^{7,8,17} While in the ligand-free state of the domain the N-terminal 14 residue sequence is unstructured, it becomes ordered forming an amphipathic α-helix (helix 0 or α0) upon binding to PtdIns(4,5)P₂ or Ins(1,4,5)P₃, a head group of the lipid.^{7,8} Binding of the ENTH domain to PtdIns(4,5)P₂ facilitates deformation of the membrane due to the insertion of α0 into the membrane interior, pushing the headgroups apart and reducing the energy barrier of bending.^{8,9} The ENTH-like AP180

N-terminal homology (ANTH) domain is nearly twice as large, consisting of 280 residues that form ten α-helices; however, it bears a similar topology to the ENTH domain.^{6,18} In fact, the ANTH domain structure includes N-terminal α-helices of the ENTH domain followed by three additional α-helices.

Despite the structural and functional similarity, the ENTH and ANTH domains bind PtdIns(4,5)P₂ in a different manner. The Arg7, Arg8 and Lys11 of α0, Arg25 of α1, Arg63 of α3, Lys69, and His73 of α4 in the ENTH domain form a deep basic pocket that accommodates the negatively charged headgroup of PtdIns(4,5)P₂.⁸ In contrast, the ANTH domain coordinates PtdIns(4,5)P₂ via the solvent exposed Lys28 of α1, and Lys38, Lys39, Lys40 and His41 of α2.⁶ These surface residues are highly conserved in the ANTH domain distinguishing it from the ENTH domain, in which this region is neither conserved nor is it involved in the binding to PtdIns(4,5)P₂.

Here we demonstrate that anchoring of the ENTH and ANTH domains to PtdIns(4,5)P₂-enriched membranes is pH dependent and is enhanced by the acidic environment. The pH sensitivity is due to the conserved histidine residues located in the PtdIns(4,5)P₂ binding pockets and involved in the inositol headgroup coordination. Our results, derived from *in vitro* experiments using monolayer penetration, nuclear magnetic resonance (NMR), surface plasmon resonance (SPR) and liposome binding assays, combined with the mutagenesis data and *in vivo* localization of fluorescently tagged proteins, provide new insights into the multivalent mechanism of membrane docking by the ENTH and ANTH domain-containing proteins. The pH-dependent recognition of PtdIns(4,5)P₂ by the ENTH and ANTH domains is reminiscent to the pH-dependent binding of the FYVE domain to PtdIns(3)P-enriched bilayers suggesting a common regulatory mechanism of membrane anchoring by a subset of PI-binding domains.

Results and Discussion

Targeting of the ENTH and ANTH domains to PtdIns(4,5)P₂-containing bilayers is pH-dependent

To understand the role of physiological pH alterations on the ability of the ENTH and ANTH domains to associate with PtdIns(4,5)P₂-containing membranes, the protein–lipid interactions in a range of pH values were investigated by liposome binding assays. The glutathione S-transferase (GST)-fusion ENTH and ANTH domains were incubated with small unilamellar vesicles (SUVs) composed of lipids normally found in plasma membranes including phosphatidylcholine (PC), phosphatidylethanolamine (PE) and PtdIns(4,5)P₂ at pH 6.0, 7.0 or 8.0. Following the centrifugation, the partitioning of proteins between supernatant and pelleted fraction was examined. As demonstrated in Figure 1(a) and

(b) one-third of the ENTH domain and a half of the ANTH domain retained in the pelleted liposome fraction at a low pH of 6.0. At each progressively higher pH value, both domains were increasingly redistributed to the supernatant. The densitometry analysis of the gel bands revealed that binding to PtdIns(4,5)P₂-enriched vesicles was reduced from 36% to 19% for the ENTH domain and from 63% to 46% for the ANTH domain as a result of alkalization of the buffer from pH 6.0 to 8.0 (Figure 1(a) and (e)). The GST tag alone was found in the soluble fraction in all buffers tested indicating that it is the ENTH and ANTH domains that bind PtdIns(4,5)P₂-containing liposomes in a pH-dependent manner (Figure 1(c)). In the absence of PtdIns(4,5)P₂, neither domain associated with SUVs, confirming that PtdIns(4,5)P₂ is required for the membrane localization of these proteins.

Affinities of the ENTH and ANTH domains for PtdIns(4,5)P₂-containing vesicles increase in the acidic environment

To quantitatively assess the effect of pH, kinetic and equilibrium binding constants of the ENTH and ANTH domains' association with bilayers were measured by SPR (Figure 2 and Table 1). We first tested binding of the Epsin ENTH domain to POPC/POPE/PtdIns(4,5)P₂ (78:20:2) vesicles at different pH values using POPC/POPE (80:20) vesicles as a control. It has been shown that in the absence of PtdIns(4,5)P₂ both domains are unable to bind liposomes even at high micromolar concentrations of the proteins.⁹ In the presence of PtdIns(4,5)P₂, the ENTH domain localized to the vesicles; however,

the binding affinity was significantly decreased when pH of the buffer was raised from pH 6.0 to pH 8.0. Thus the ENTH domain exhibited a 9.8 nM affinity for POPC/POPE/PtdIns(4,5)P₂ vesicles at pH 6.0; however, this interaction was eightfold weaker at pH 7.4 and 34-fold weaker at pH 8.0 (Table 1). Concurrently a decrease of k_a and an increase of k_d were observed, most likely due to the reduced electrostatic interactions and a lesser degree of membrane penetration by the ENTH domain.^{19,20}

A similar enhancement of the membrane binding affinity upon acidification was seen for the AP180 ANTH domain. We monitored the ANTH domain association with PtdIns(4,5)P₂-containing vesicles at pH 6.0, 7.4, and 8.0. Since the k_d value of this interaction at pH 8.0 was too fast to measure accurately, the affinity was assessed by equilibrium binding analysis (Table 1). As expected the ANTH domain displayed a significant increase in affinity in acidic conditions and a decrease in basic. The K_d value of the ANTH domain association with POPC/POPE/PtdIns(4,5)P₂ vesicles was found to be 95 nM at pH 6.0. This binding was reduced by fivefold and 13-fold at pH 7.4 and pH 8.0, respectively (Table 1). Thus our data demonstrate that pH mediates docking of the Epsin ENTH and AP180 ANTH domains to PtdIns(4,5)P₂-containing bilayers.

The cytosolic pH can regulate sub-cellular localization of the Epsin ENTH and AP180 ANTH domains

To examine the role of intracellular pH for *in vivo* localization of the proteins, enhanced green

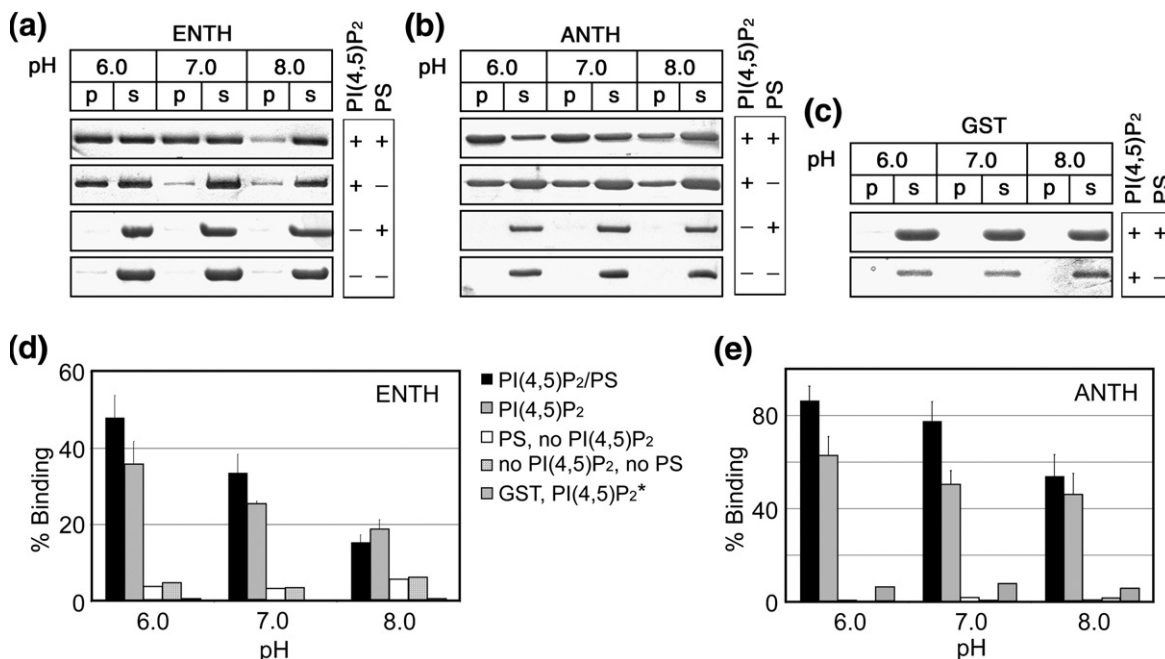


Figure 1. pH-dependent binding of the Epsin ENTH and AP180 ANTH domains to PtdIns(4,5)P₂-enriched liposomes. The SDS-PAGE gels ((a) – (c)) and histograms ((d) and (e)) show partitioning of the ENTH and ANTH domains between supernatant (s) and the liposome pellet (p) at indicated pH values. (*) Association of GST with PC/PE/PtdIns(4,5)P₂ vesicles in the absence (d) and presence (e) of PS. The experimental points were averaged over at least three measurements.

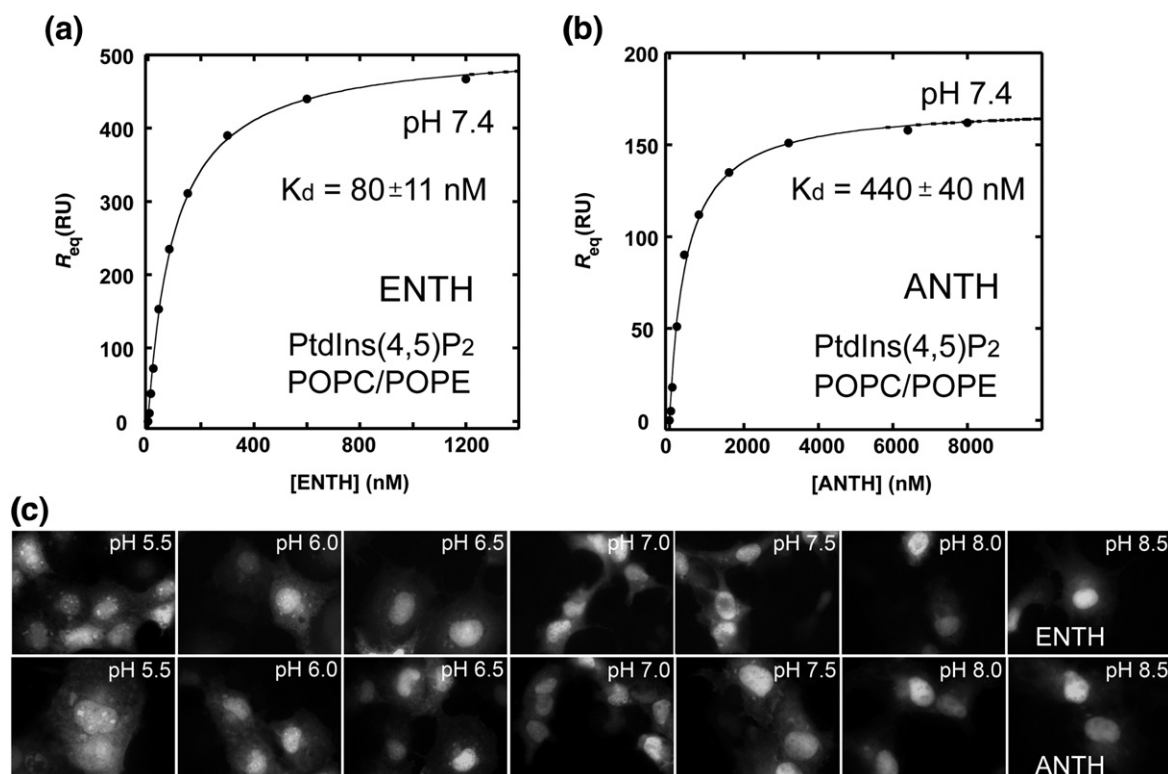


Figure 2. Affinities of the ENTH and ANTH domains for PtdIns(4,5)P₂-containing membranes increase in the acidic environment. (a) and (b) SPR measurements used to determine K_d values of the ENTH and ANTH domains association with POPC/POPE/PtdIns(4,5)P₂ vesicles. The continuous line represents a theoretical curve obtained based on R_{max} and K_d values determined by non-linear least-squares analysis. (c) Changes in localization of EGFP-ENTH and EGFP-ANTH domains in COS-1 cells upon varying the cytosolic pH. Cultures were incubated in solutions buffered to the indicated pH values for 15 min. The cells were visualized by fluorescence microscopy.

fluorescent protein (EGFP)-fusion Epsin ENTH and AP180 ANTH domains were expressed in COS-1 cells that were briefly incubated in media buffered to various pH values (Figure 2(c)). Mammalian cells

maintain an intracellular pH of approximately pH 7.3;²¹ however, the neutral nature of the cytosol can be altered by changing the pH of the medium.²² We investigated the sub-cellular distribution of EGFP-

Table 1. Binding properties of the Epsin ENTH and AP180 ANTH domains and Epsin H73A mutant

Protein	k_a ($M^{-1} s^{-1} \times 10^5$)	k_d ($s^{-1} \times 10^{-2}$)	K_d ($M \times 10^{-9}$)	Fold change ^a
<i>POPC/POPE/PtdIns(4,5)P₂</i> (78:20:2)				
ENTH (pH 6.0)	(8.2±0.6)	(0.80±0.07)	(9.8±1.0)	–
H73A ENTH (pH 6.0)	(5.8±0.4)	(2.8±0.3)	(48±6)	5
ENTH (pH 7.4)	(4.4±0.5)	(3.5±0.3)	(80±11)	8
H73A ENTH (pH 7.4)	(2.4±0.3)	(5.9±0.4)	(250±36)	26
ENTH (pH 8.0)	(1.9±0.2)	(6.2±0.4)	(330±60)	34
H73A ENTH (pH 8.0)	(1.0±0.2)	(9.3±0.5)	(930±190)	95
ANTH (pH 6.0)	–	–	(95±12)	–
ANTH (pH 7.4)	–	–	(440±40)	5
ANTH (pH 8.0)	–	–	(1200±120)	13
<i>POPC/POPE/POPS/PtdIns(4,5)P₂</i> (63:20:15:2)				
ENTH (pH 6.0)	(9.7±0.6)	(0.25±0.03)	(2.6±0.3)	–
H73A ENTH (pH 6.0)	(8.0±0.5)	(0.81±0.04)	(10±0.8)	4
ENTH (pH 7.4)	(9.2±0.4)	(1.8±0.2)	(20±2.4)	8
H73A ENTH (pH 7.4)	(6.8±0.6)	(3.6±0.3)	(53±6)	20
ENTH (pH 8.0)	(4.5±0.5)	(3.1±0.3)	(69±10)	26
H73A ENTH (pH 8.0)	(3.5±0.4)	(5.8±0.5)	(170±24)	65
ANTH (pH 6.0)	–	–	(18±4)	–
ANTH (pH 7.4)	–	–	(98±12)	5
ANTH (pH 8.0)	–	–	(290±40)	16

^a Decrease of the affinity relative to the K_d of wild-type ENTH at pH 6.0.

ENTH and EGFP-ANTH at pH 5.5, 6.0, 6.5, 7.0, 7.5, 8.0 and 8.5 by fluorescence microscopy. In media buffered to pH 5.5–6.5, both EGFP-ENTH and EGFP-ANTH were found in membrane microdomains and the nucleus (Figure 2(c)).^{17,23} When pH of the media was gradually increased, the EGFP signal of the microdomain-associated ENTH and ANTH domains was diminished and an increase in the nuclear EGFP signal was observed. In basic conditions only a nuclear pool of EGFP-ENTH and EGFP-ANTH was detected. The most significant changes in the ENTH and ANTH domains' localization occurred in the physiological pH range of pH 6.5 to pH 7.5. Thus, the Epsin ENTH domain and AP180 ANTH domain localize to the membrane microdomains and the nucleus at low cytosolic pH, whereas at high pH values the proteins are found primarily in the nucleus.

PtdIns(4,5)P₂ binding of the ENTH and ANTH domains is pH-sensitive

To test whether the pH dependence is attributed to the direct interaction of the ENTH or ANTH domain with PtdIns(4,5)P₂, the protein-lipid binding was characterized in the absence of membrane-mimetics by PIP₂-pull down assays and NMR spectroscopy. The GST-fusion ENTH and ANTH domains were incubated with PtdIns(4,5)P₂ immobilized beads at pH 6.0, 7.0 and 8.0 and association with the lipid was examined by sedimentation and SDS-PAGE and quantified by densitometry (Figure 3(a) and (b)). Both ENTH and ANTH domains showed a steady decrease in binding to PIP₂-beads when pH was raised from pH 6.0 to pH 8.0, indicating that

the PtdIns(4,5)P₂ interaction of these modules is indeed pH-sensitive and is enhanced by the acidic media.

The enhancement of PtdIns(4,5)P₂ binding in a low pH environment was substantiated by resonance perturbations seen in NMR spectra of the Epsin ENTH domain. We collected ¹H-¹⁵N heteronuclear single quantum coherence (HSQC) spectra of the uniformly ¹⁵N-labeled protein at pH 6.0, 6.6 and 8.0 as soluble C₄-PtdIns(4,5)P₂ lipid was gradually added. As demonstrated in Figure 3(c), progressive changes in the amide resonances of the ENTH domain were observed at pH 6.0; however, at pH 8.0 an excess of PtdIns(4,5)P₂ induced barely any chemical shift perturbations, implying that the binding affinity is low under basic conditions. The fast exchange on the NMR time-scale also suggested that the ENTH domain binds water-soluble short chain C₄-PtdIns(4,5)P₂ weaker than the long chain lipid embedded in the vesicles (Table 1 and Figure 3(c)). Taken together our data indicate that the direct interaction of the ENTH and ANTH domains with PtdIns(4,5)P₂ lipid is pH dependent and becomes stronger under the acidic conditions.

Conserved His73 residue of the ENTH domain mediates PtdIns(4,5)P₂ binding

Our previous studies revealed that PtdIns(3)P binding of the FYVE domain is modulated by the protonation state of His residues.²⁴ The PtdIns(4,5)P₂ binding pocket of the ENTH domain contains a conserved His73 residue which forms a hydrogen bond to the 4-phosphate group of PtdIns(4,5)P₂ as seen in the crystal structure of the Epsin ENTH

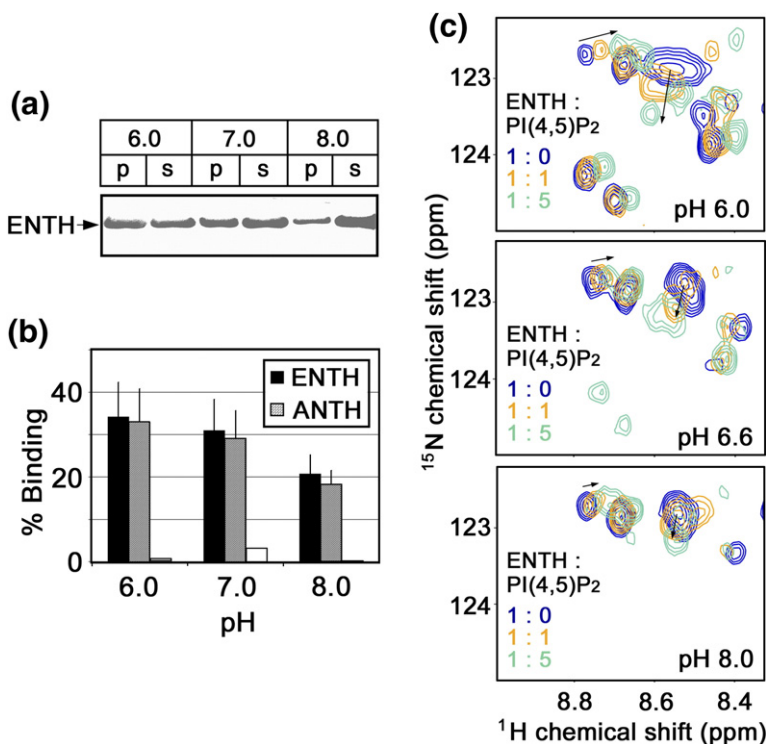


Figure 3. The direct interaction of the ENTH and ANTH domains with PtdIns(4,5)P₂ is pH-sensitive and is enhanced by lowering the pH. (a) The SDS-PAGE gel and (b) histogram display the distribution of the ENTH and ANTH domains between supernatant (s) and pelleted PIP₂-beads (p) at indicated pH values. (c) Superimposed ¹H-¹⁵N HSQC spectra of the ¹⁵N-labeled ENTH domain (0.2 mM) recorded during addition of C₄-PtdIns(4,5)P₂ at pH 6.0, 6.6 and 8.0. The relative concentrations of the ENTH domain and the lipid [PI(4,5)P₂] are color-coded.

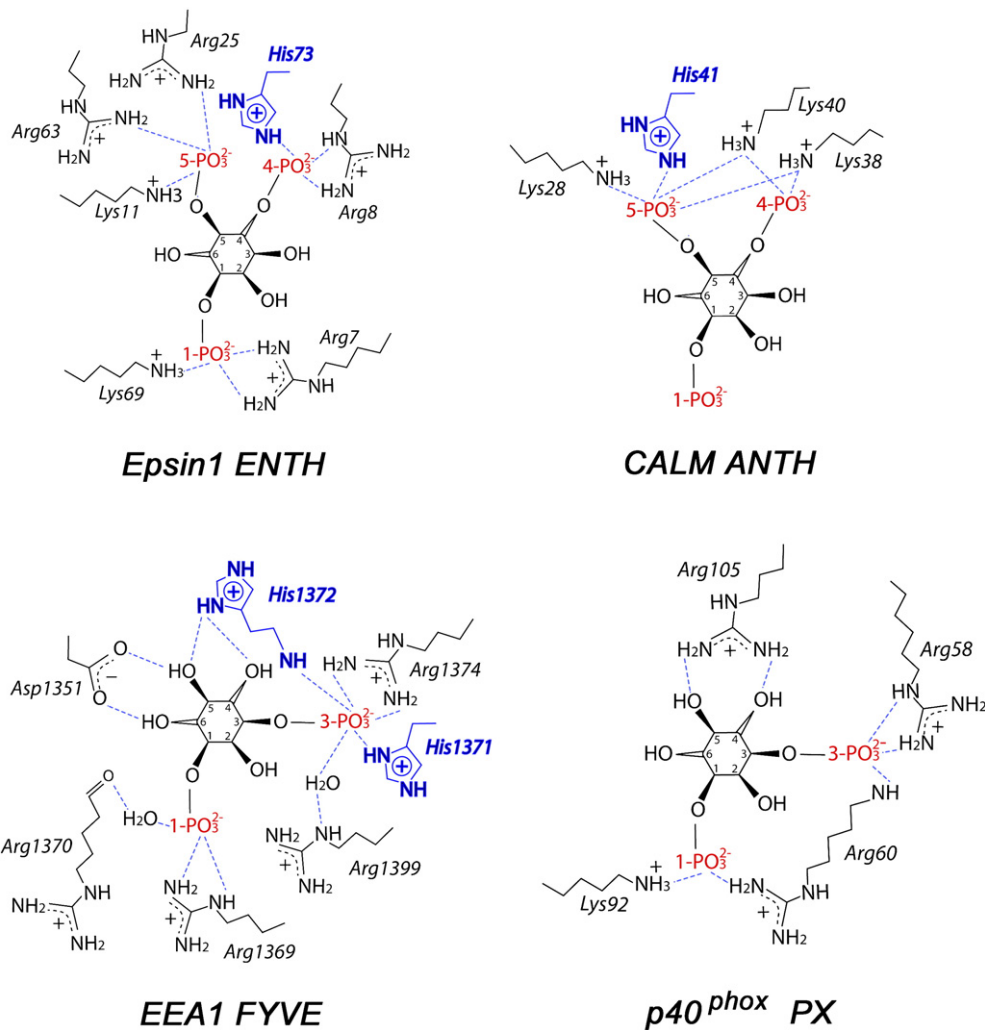


Figure 4. Schematic diagrams showing PtdIns(4,5)P₂ headgroup coordination by Epsin ENTH and CALM ANTH domains, and PtdIns(3)P headgroup coordination by EEA1 FYVE and p40^{phox} PX domains (PDB codes 1HOA, 1HFA, 1JOC and 1H6H). Only charged residues of the proteins are depicted for clarity.

domain (Figures 4 and 5).⁸ To determine whether His73 plays a role in the pH-dependent membrane anchoring it was replaced with Ala and binding of the H73A mutant protein to POPC/POPE/PtdIns(4,5)P₂ vesicles was probed at different pH values. We found that the H73A mutant associates with vesicles fivefold weaker than the wild-type ENTH domain at pH 6.0, threefold weaker at pH 7.4 and 2.8-fold weaker at pH 8.0 (Table 1). Overall, when compared to the affinity of the mutant measured at pH 6.0, the binding affinity of H73A was decreased by fivefold at pH 7.4 and 20-fold at pH 8.0. In contrast, the wild-type ENTH domain showed an eight- and 34-fold decrease in the affinity at pH 7.4 and pH 8.0, respectively. Thus our data indicate that His73 is necessary for the strong membrane anchoring and its protonation increases the binding affinity.

The fact that the H73A mutant did not entirely abolish the interaction indicates that the binding site lysine and arginine residues play a key role in coordinating the lipid (Figures 4 and 5).

Furthermore, mutation of His73 decreases the pH sensitivity of binding but does not eliminate it, suggesting that other His residues may be responsible for the remaining pH dependence. Thus, the surface residues His15 and His68 of the ENTH domain and His32 of the ANTH domain are located in close proximity to the PtdIns(4,5)P₂ binding site and may contribute to the interactions with acidic membranes (Figure 5). It may also indicate the existence of another concomitantly occurring process, i.e. deprotonation of PtdIns(4,5)P₂ in basic conditions. The pK_a values of the 4- and 5-phosphate groups are estimated to be 6.7 and 7.6;²⁵ therefore in the physiological pH range the net charge of PtdIns(4,5)P₂ undergoes a substantial change from -3 (pH < 6.0) to -5 (pH > 8.0). The basic environment promotes deprotonation of both phosphate groups resulting in complete ionization of this phospholipid and accumulation of two extra negative charges. On the contrary to deprotonation of His73, this should strengthen PtdIns(4,5)P₂ coordination by

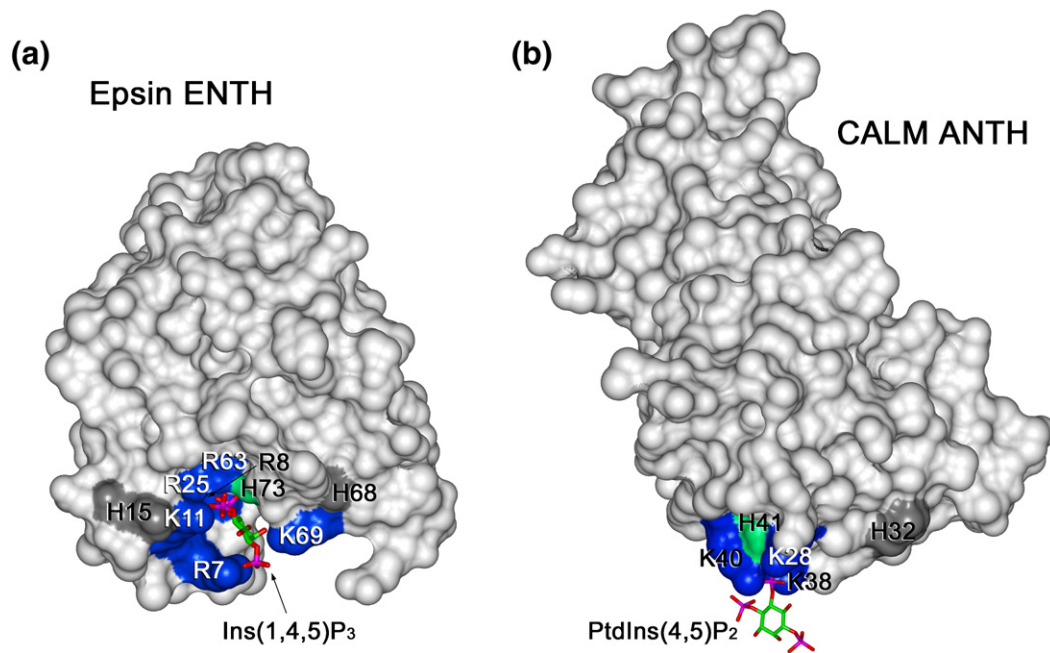


Figure 5. PtdIns(4,5)P₂ binding pocket defined from the crystal structure of the Epsin ENTH domain complexed with Ins(1,4,5)P₃ (PDB code 1HOA) (a) and the crystal structure of the CALM ANTH domain in complex with PtdIns(4,5)P₂ (PDB code 1HFA) (b). The basic binding site residues are labeled and colored blue. The conserved His73 of the Epsin ENTH domain and His41 of the ANTH domain are in green. Other surface His residues are in gray.

the positively charged lysine and arginine residues of the ENTH domain.

Non-specific electrostatic interactions with PS enhance the ENTH and ANTH domain binding to PtdIns(4,5)P₂-containing vesicles

The inner leaflet of the plasma membrane contains over 10% of anionic phospholipids such as PS and PI.²⁶ To determine whether non-specific electrostatic interactions with acidic lipids other than PtdIns(4,5)P₂ contribute to the pH dependent behavior of the ENTH and ANTH domains, liposome binding assays were carried out using PC/PE/PS/PtdIns(4,5)P₂ vesicles. As shown in Figure 1(d) and (e), both domains bound PS-containing vesicles better than the neutral vesicles at all pH values tested. In the presence of PS, the fraction of the liposome-bound ENTH and ANTH domains increased from 36% to 50% and from 63% to 90%, respectively, suggesting that non-specific electrostatic interactions with PS amplify the binding affinity. The pH sensitivity of the ENTH and ANTH domains toward PS-containing vesicles was clearly preserved (Figure 1(d) and (e)).

To further assess the effect of PS, we measured kinetic and thermodynamic parameters of the ENTH and ANTH binding to POPC/POPE/POPS/PtdIns(4,5)P₂ (63:20:15:2) vesicles (Table 1). The ENTH domain exhibited an increase in affinity at all pH levels when PS was present. At pH 6.0 the protein was bound with nearly fourfold higher affinity to PS-enriched vesicles than to the vesicles without PS, demonstrating the significance of non-

specific electrostatic interactions for membrane targeting. Furthermore, the ENTH domain displayed the same fourfold increase in the affinity at pH 7.4 and pH 8.0, indicating similar contributions of non-specific electrostatic interactions. This was further supported by examining the binding of H73A to POPC/POPE/POPS/PtdIns(4,5)P₂ vesicles at different pHs. The H73A mutant showed a fivefold higher affinity for PS-containing vesicles than those without this lipid at any pH. A comparable four- to fivefold increase of the affinity was observed for the ANTH domain association with POPC/POPE/POPS/PtdIns(4,5)P₂ vesicles across the pH range tested. This again demonstrates that non-specific electrostatic interactions are essential for membrane recruitment of the AP180 ANTH domain.

Membrane insertion of the ENTH domain is promoted by acidic pH

Recent reports have demonstrated that the ENTH domain penetrates PtdIns(4,5)P₂-enriched membranes by inserting helix 0 into the bilayer.^{8,9} In contrast, the ANTH domain lacking exposed hydrophobic residues near the PtdIns(4,5)P₂ binding interface does not penetrate and interacts with membranes through a bridging model (Figure 5). To examine the effect of the pH on the membrane insertion we tested both proteins by monolayer penetration experiments. Phospholipid monolayers at the air-water interface serve as a highly sensitive tool for measuring the membrane penetrating ability of peripheral proteins.^{9,20,27,28} POPC/POPE (80:20)

or POPC/POPE/PtdIns(4,5)P₂ monolayers of a given initial surface pressure (π) were spread at a constant area and the change in surface pressure after the injection of proteins was monitored. $\Delta\pi$ is inversely proportional to π and an extrapolation of $\Delta\pi$ versus π yields the critical surface pressure π_{χ} , which specifies an upper limit of π that a protein can penetrate into.²⁹ Because the surface pressure of cell membranes and large unilamellar vesicles is estimated to be in a range of 30 dyne/cm – 35 dyne/cm,^{20,28} for a protein to penetrate these bilayers its π_{χ} value should be above 30 dyne/cm.

Figure 6(a) shows that both Epsin ENTH and AP180 ANTH domains have low intrinsic penetrating ability toward a POPC/POPE monolayer and the π_{χ} values (21 and 25 dyne/cm) remain essentially unchanged when the experiments were performed at pH 6.0, 7.4 or 8.0. Thus, in the absence of PtdIns(4,5)P₂ the ENTH and ANTH domains do not penetrate POPC/POPE membranes nor does the pH influence the insertion. We next examined the penetration of the Epsin ENTH domain into PtdIns(4,5)P₂ containing monolayers at different pH levels (Figure 6(b)). When 3 mol% PtdIns(4,5)P₂ was incorporated in the monolayer, the ENTH domain penetration increased to 27 dyne/cm at pH 8.0. Furthermore, the π_{χ} value rose to 31 dyne/cm and 34.5 dyne/cm at pH 7.4 and pH 6.0, respectively, indicating that the acidic environment enhances not only the membrane affinity but also the penetrating capability of the ENTH domain. Based on the

estimated π_{χ} values, the ENTH domain should not significantly penetrate biological membranes at above pH 7.4. Unlike the wild-type protein, H73A mutant lost the pH dependency (Figure 6(c)). In fact, it had much lower penetrating power than the wild-type ENTH at pH 6.0 and pH 7.4; however, similarly to the wild-type protein, H73A was unable to effectively insert into the monolayer at pH 8.0. These data confirm the critical role of His73 in PtdIns(4,5)P₂ binding and further support the notion that the membrane penetration of the ENTH domain requires efficient PtdIns(4,5)P₂ binding which in turn is induced by the acidic media.

Our recent studies show that the AP180 ANTH domain binds PtdIns(4,5)P₂ containing vesicles primarily through electrostatic interactions and does not penetrate the bilayers.²⁷ To rule out the possibility that pH influences the penetration of the ANTH domain, we monitored its binding to POPC/POPE/PtdIns(4,5)P₂ monolayers at different pH values (Figure 6(d)). Although the ANTH domain bound PtdIns(4,5)P₂ containing membranes much stronger at pH 6.0, we did not observe an increase in monolayer penetration. Likewise, no significant penetration into PtdIns(4,5)P₂ containing monolayers was seen at pH 7.4 or pH 8.0. This and the data described above corroborate that PtdIns(4,5)P₂ recognition of the ANTH domain is pH-dependent but the higher affinity in acidic conditions is not caused by changes in the membrane penetration of this module.

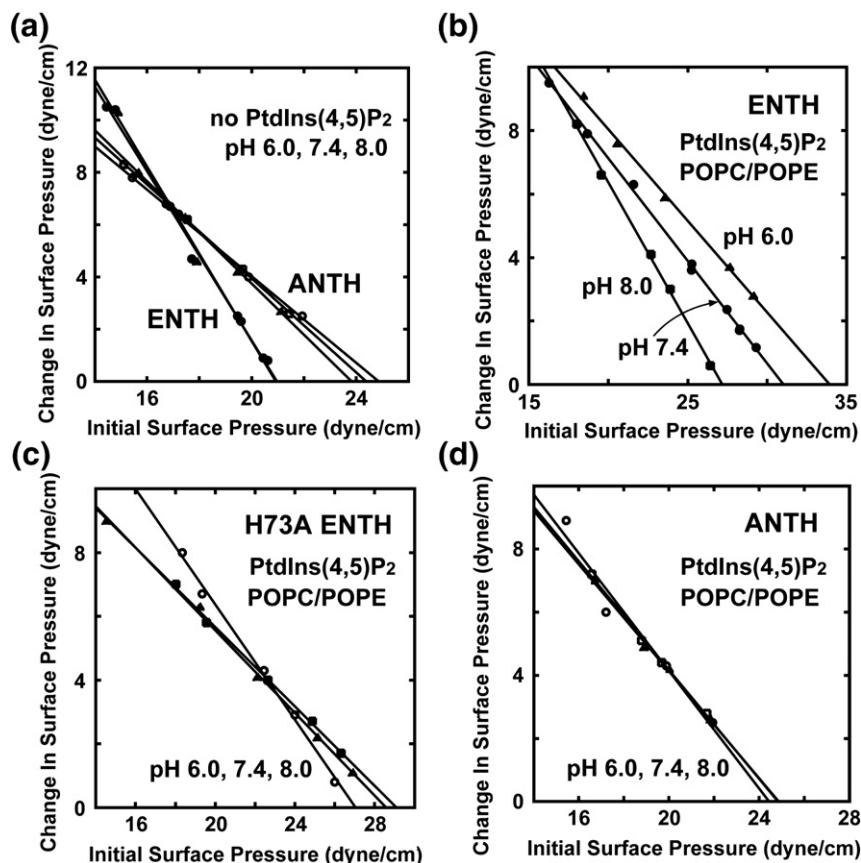


Figure 6. Monolayer penetration of Epsin ENTH and AP180 ANTH domains. (a) Insertion of wild-type ENTH (filled symbols) and ANTH (open symbols) into a POPC/POPE (80:20) monolayer at pH 6.0 (triangle), pH 7.4 (circle) and pH 8.0 (square) monitored as a function of π_0 . (b) Penetration of wild-type ENTH and (c) H73A ENTH into a POPC/POPE/PtdIns(4,5)P₂ (77:20:3) monolayer at pH 6.0 (triangle), pH 7.4 (circle) and pH 8.0 (square). (d) Penetration of AP180 ANTH into a POPC/POPE/PtdIns(4,5)P₂ (77:20:3) monolayer at pH 6.0 (triangle), pH 7.4 (circle) and pH 8.0 (square).

Conclusions

Our results reveal a pH-dependent mechanism of membrane docking by the Epsin ENTH and AP180 ANTH domains. At the core of this mechanism is the ability of His residues involved in PtdIns(4,5)P₂ coordination to undergo a rapid protonation/deprotonation transition in the physiological pH range, and thus modulate the strength of the lipid binding (Figures 4 and 5). The acidic environment causes protonation of essential His73 and His41 residues of the ENTH and ANTH domains, which in turn facilitates binding of these proteins to PtdIns(4,5)P₂. Alignment of the ENTH and ANTH domain sequences shows conservation of both His residues (Figure 7), suggesting that pH-dependent membrane association may be a general characteristic of these modules.

The pH dependent recognition of PtdIns(4,5)P₂ by the ENTH and ANTH domains resembles the pH sensitivity of the FYVE finger.²⁴ Because of a single His residue, however, they display much weaker pH dependence than the FYVE domain, which contains two adjacent His residues in the PtdIns(3)P binding site and exhibits sharp pH dependency (Figure 4). The pH-sensitive function of the ENTH, ANTH and FYVE domains suggests a common anchoring mechanism for a subset of PI-binding modules, distinguishing them from the PX domain, which contains no histidine residues in the PI-binding pocket and is shown to be pH independent.²⁴

The pH-dependence can influence the functions of Epsin and AP180 in cells with unusual cytosolic pH levels and in normal cells during physiological processes that involve changing of pH. Intracellular pH often fluctuates in response to cell growth, development, and apoptosis, with pH varying from pH 6.3 to pH 7.8.^{30–33} Even wider fluctuations are detected in anomalous cells during ischemia,³⁴ inflammation³⁵ and cancer.³⁶ We found that EGFP–Epsin ENTH and AP180 ANTH asso-

ciation with membrane micro-domains is diminished when the intracellular pH is increased. This suggests that sub-cellular localization of the ENTH and ANTH domains can vary due to fluctuations in acidification or alkalization of the cytosol. Future studies are required to establish the significance of the pH sensing by the ENTH and ANTH domains and to determine whether the membrane localization of these proteins is altered in biological processes that are accompanied by the changes in cytosolic pH.

Methods

Sub-cloning, expression and purification of proteins

Human AP180 ANTH domain (residues 1–289) and rat Epsin ENTH domain (residues 1–164 and 1–144) were expressed in *Escherichia coli* BL21 (DE3) pLysS strain in LB or in ¹⁵NH₄Cl supplemented minimal media (Isotec). Bacteria were harvested by centrifugation after induction with IPTG (0.1 mM) and lysed using a French press (18,000 lb/in², at 4 °C). The unlabeled or ¹⁵N-uniformly labeled GST-fusion proteins were purified on a glutathione Sepharose 4B column (Amersham). The GST tag was cleaved with thrombin (Sigma). The proteins were concentrated using Millipore concentrators (Millipore) and purified by FPLC. The buffer was exchanged into 20 mM Tris or perdeuterated (d)₁₁-Tris, 150 mM KCl, 1 mM d₁₀-dithiothreitol, 50 μM 4-amidinophenylmethane sulfonyl fluoride and 7% ²H₂O. The purity of the proteins was determined by SDS-PAGE and ¹H NMR.

PCR mutagenesis

Site-directed mutagenesis of Epsin ENTH domain was performed using a QuikChange kit (Stratagene). The sequence of the H73A ENTH construct was confirmed by DNA sequencing.

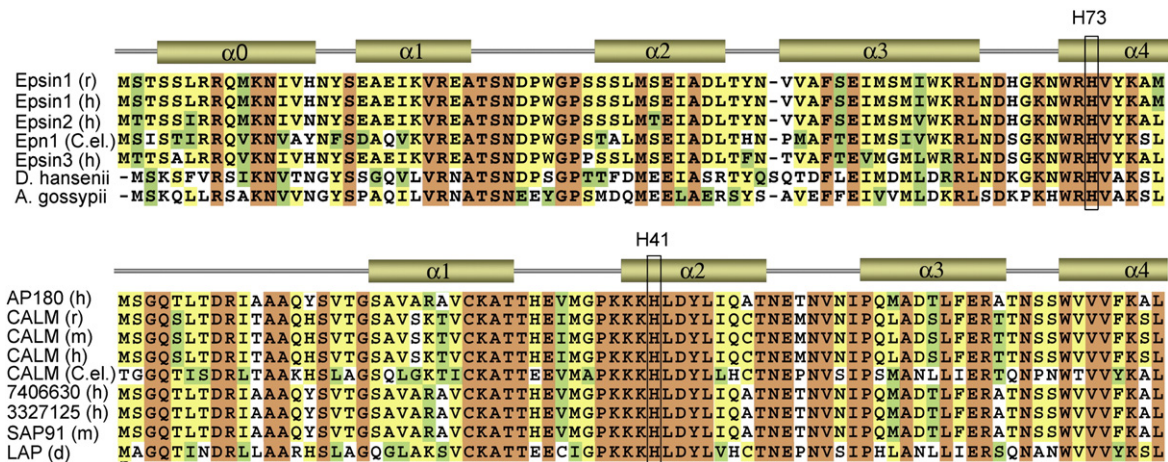


Figure 7. Alignment of the ENTH and ANTH domain sequences: absolutely, moderately and weakly conserved residues are colored brown, yellow and green, respectively. The secondary structure is shown above the sequences (only the N-terminal part of the domains is depicted). The conserved His73 residue of the ENTH domain and His41 of the ANTH domain are labeled.

Liposome binding

The liposome binding assays were performed as described.²⁴ Briefly, solutions of PC, PE, PS (Avanti) and C₁₆-PtdIns(4,5)P₂ (Echelon Biosciences Inc.) dissolved in CHCl₃/MeOH/H₂O (65:25:4, by volume) were mixed and dried down under vacuum. The lipids were resuspended in 50 mM Tris, 100 mM KCl (pH 7.0) and incubated at 64 °C for 1 h. The liposomes were then frozen in liquid nitrogen and thawed at 37 °C for three cycles. The liposome solution was passed through an Avanti extruder to produce 1.0 μm liposomes. Liposomes were collected by centrifugation at 25,000g for 10 min and resuspended to a final concentration of 2 mM total lipids in 100 μl 20 mM Tris, 100 mM KCl buffer (pH 6.0, 7.0 or 8.0). Liposomes were incubated with the GST-fusion ENTH and ANTH domains or GST (2–5 μg/ml final protein concentration) for 30 min at room temperature and then collected again by centrifugation. The liposome pellets were resuspended in 100 μl of buffer and analyzed by SDS-PAGE and Coomassie brilliant blue staining.

PIP2-Beads pull-down

The 2–5 μg ENTH domain, ANTH domain or GST were incubated with 100 μl of PIP2 beads (Echelon Biosciences Inc.) suspended in bis-Tris or Tris (pH 6.0, 7.0 or 8.0) buffers at room temperature for 1 h. The beads fraction and supernatant were separated by centrifugation and analyzed by SDS-PAGE.

NMR spectroscopy and lipid titrations

NMR spectra were recorded at 25 °C on a Varian INOVA 500 MHz spectrometer. The ¹H-¹⁵N HSQC spectra of 0.2 mM uniformly ¹⁵N-labeled ENTH domain were collected using 1024 t₁ increments of 2048 data points, 96 number of increments and spectral widths of 7500 Hz and 1367 Hz in the ¹H and ¹⁵N dimensions, respectively. PtdIns(4,5)P₂ binding was characterized at pH 6.0, 6.6 and 8.0 by monitoring chemical shift changes in ¹H-¹⁵N HSQC spectra of the ENTH domain as soluble C₄-PtdIns(4,5)P₂ was added stepwise up to 1 mM.

Monolayer measurements

Insertion of the ENTH and ANTH domains into a monolayer was investigated by measuring a change in the surface pressure (π) of invariable surface area during addition of the proteins. The experiments were performed using a 1 ml circular Teflon trough and wire probe connected to a Kibron MicroTrough X (Kibron, Inc., Helsinki). A lipid monolayer containing various combinations of phospholipids was spread onto the sub-phase composed of either 10 mM KH₂PO₄ and 0.16 M KCl at (pH 6.0) or 10 mM Hepes and 0.16 M KCl (at pH 7.4 and pH 8.0) until the desired initial surface pressure (π_i) was reached. After the signal stabilized (~5 min), 10 μg of protein was injected into the sub-phase through a hole in the wall of the trough. The change in surface pressure ($\Delta\pi$) was monitored for 45 min. The $\Delta\pi$ value reached a maximum after 30 min in all experiments. The resulting $\Delta\pi$ was plotted *versus* π_i , and critical surface pressure (π_x) was determined as the x -intercept.

Surface plasmon resonance (SPR)

The SPR experiments were performed at 25 °C as described.¹⁹ Kinetic SPR measurements were carried out at a flow rate of 30 μl/min. After 90 μl of the protein in a particular pH buffer was injected, the association and dissociation were monitored for 90 s and over 500 s, respectively. The sensorgrams were obtained using five or more different concentrations of each protein within a tenfold range of K_d and corrected for refractive index change by subtracting the control surface response. The association and dissociation phases of sensorgrams were globally fit to a 1:1 Langmuir binding model: protein + (protein binding site on vesicle) ↔ (complex) using BIAevaluation software (Biacore) as described.¹⁹ The dissociation constant (K_d) was calculated from the equation $K_d = k_d/k_a$. Each data set was repeated three times to obtain a standard deviation value. Mass transport³⁷ was not a limiting factor in these experiments, since the change in a flow rate from 3 μl/min to 90 μl/min did not affect kinetics of association and dissociation. To verify the binding model, residual plots and χ^2 values were examined. Equilibrium binding measurements were performed at a 5 μl/min flow rate. The maximum response (R_{eq}) for each protein concentration was determined and plotted *versus* protein concentrations (C). The K_d value was determined by a non-linear least-squares analysis of the binding isotherm using the equation $R_{eq} = R_{max}/(1 + K_d/C)$.²⁰

The *in vivo* localization of enhanced green fluorescent protein (EGFP)-fusion Epsin ENTH and AP180 ANTH domains

COS-1 cells were grown in Dulbecco Modified Essential Medium (DMEM) (Mediatech) supplied with 10% (v/v) fetal bovine serum (Invitrogen). The cells were plated on 25 mm glass coverslips and transfected with pEGFP-ANTH and pEGFP-ENTH using Effectene reagent (Qiagen). Cell imaging was performed 48–60 h after transfection. Before imaging, cells were rinsed twice with phosphate buffered saline (PBS; 137 mM NaCl, 2.7 mM KCl, 4.3 mM Na₂HPO₄, 1.4 mM KH₂PO₄ (pH 7.4)) followed by addition of buffered solutions containing 10 μg/ml of nigericin (Sigma) and 10 μg/ml of monensin (Sigma). The buffered solutions contained 120 mM KCl, 20 mM NaCl, 0.5 mM CaCl₂, 0.5 mM MgSO₄, and phosphate or biphthalate buffers of pH 5.5–8.5. After equilibration for 15 min at 37 °C, cells were fixed with 4% (v/v) paraformaldehyde (Electron Microscopy Sciences) for 30 min at room temperature, rinsed once with the corresponding buffered solution and twice with PBS followed by permeabilization with 0.1% (w/v) saponin (Acros Organics) in PBS for 10 min. The cells were then visualized on Olympus IX81 inverted microscope equipped with 60× oil immersion objective lens and a FITC filter set (Chroma), and operated by IPLab (v. 4.0) software (BD Biosciences).

Acknowledgements

We thank C. Burd, P. DeCamilli and A. Sorkin for discussions, P. DeCamilli and H. McMahon for providing cDNAs of the ENTH and ANTH domains

and S. Lee for sub-cloning and mutagenesis. This research was supported by grants from the National Institutes of Health, GM070358 and GM073913 (to V.V.V.) and GM071424 and CA113472 (to T.G.K.) and an Indiana University Biomedical Research Grant (to R.V.S.).

References

1. Brodsky, F. M., Chen, C. Y., Knuehl, C., Towler, M. C. & Wakeham, D. E. (2001). Biological basket weaving: formation and function of clathrin-coated vesicles. *Annu. Rev. Cell. Dev. Biol.* **17**, 517–568.
2. Sorkin, A. & Von Zastrow, M. (2002). Signal transduction and endocytosis: close encounters of many kinds. *Nature Rev. Mol. Cell. Biol.* **3**, 600–614.
3. Marsh, M. & McMahon, H. T. (1999). The structural era of endocytosis. *Science*, **285**, 215–220.
4. Cremona, O. & De Camilli, P. (2001). Phosphoinositides in membrane traffic at the synapse. *J. Cell Sci.* **114**, 1041–1052.
5. Slepnev, V. I. & De Camilli, P. (2000). Accessory factors in clathrin-dependent synaptic vesicle endocytosis. *Nature Rev. Neurosci.* **1**, 161–172.
6. Ford, M. G., Pearce, B. M., Higgins, M. K., Vallis, Y., Owen, D. J., Gibson, A. *et al.* (2001). Simultaneous binding of PtdIns(4,5)P₂ and clathrin by AP180 in the nucleation of clathrin lattices on membranes. *Science*, **291**, 1051–1055.
7. Itoh, T., Koshiba, S., Kigawa, T., Kikuchi, A., Yokoyama, S. & Takenawa, T. (2001). Role of the ENTH domain in phosphatidylinositol-4,5-bisphosphate binding and endocytosis (see comment). *Science*, **291**, 1047–1051.
8. Ford, M. G., Mills, I. G., Peter, B. J., Vallis, Y., Praefcke, G. J., Evans, P. R. & McMahon, H. T. (2002). Curvature of clathrin-coated pits driven by epsin(comment). *Nature*, **419**, 361–366.
9. Stahelin, R. V., Long, F., Peter, B. J., Murray, D., De Camilli, P., McMahon, H. T. & Cho, W. (2003). Contrasting membrane interaction mechanisms of AP180 N-terminal homology (ANTH) and Epsin N-terminal homology (ENTH) domains. *J. Biol. Chem.* **278**, 28993–28999.
10. Itoh, T. & De Camilli, P. (2006). BAR, F-BAR (EFC) and ENTH/ANTH domains in the regulation of membrane-cytosol interfaces and membrane curvature. *Biochim. Biophys. Acta*, **1761**, 897–912.
11. Legendre-Guillemain, V., Wasiaik, S., Hussain, N. K., Angers, A. & McPherson, P. S. (2004). ENTH/ANTH proteins and clathrin-mediated membrane budding. *J. Cell Sci.* **117**, 9–18.
12. Rosenthal, J. A., Chen, H., Slepnev, V. I., Pellegrini, L., Salcini, A. E., Di Fiore, P. P. & De Camilli, P. (1999). The epsins define a family of proteins that interact with components of the clathrin coat and contain a new protein module. *J. Biol. Chem.* **274**, 33959–33965.
13. Kay, B. K., Yamabhai, M., Wendland, B. & Emr, S. D. (1999). Identification of a novel domain shared by putative components of the endocytic and cytoskeletal machinery. *Protein Sci.* **8**, 435–438.
14. Chen, H., Fre, S., Slepnev, V. I., Capua, M. R., Takei, K., Butler, M. H. *et al.* (1998). Epsin is an EH-domain-binding protein implicated in clathrin-mediated endocytosis. *Nature*, **394**, 793–797.
15. Drake, M. T., Downs, M. A. & Traub, L. M. (2000). Epsin binds to clathrin by associating directly with the clathrin-terminal domain. Evidence for cooperative binding through two discrete sites. *J. Biol. Chem.* **275**, 6479–6489.
16. Yamabhai, M., Hoffman, N. G., Hardison, N. L., McPherson, P. S., Castagnoli, L., Cesareni, G. & Kay, B. K. (1998). Intersectin, a novel adaptor protein with two Eps15 homology and five Src homology 3 domains. *J. Biol. Chem.* **273**, 31401–31407.
17. Hyman, J., Chen, H., Di Fiore, P. P., De Camilli, P. & Brunger, A. T. (2000). Epsin 1 undergoes nucleocytoplasmic shuttling and its eps15 interactor NH(2)-terminal homology (ENTH) domain, structurally similar to Armadillo and HEAT repeats, interacts with the transcription factor promyelocytic leukemia Zn(2)+ finger protein (PLZF). *J. Cell. Biol.* **149**, 537–546.
18. Mao, Y., Chen, J., Maynard, J. A., Zhang, B. & Quiocho, F. A. (2001). A novel all helix fold of the AP180 amino-terminal domain for phosphoinositide binding and clathrin assembly in synaptic vesicle endocytosis. *Cell*, **104**, 433–440.
19. Stahelin, R. V. & Cho, W. (2001). Differential role of ionic, aliphatic, and aromatic residues in membrane-protein interactions: a surface plasmon resonance study on phospholipases A₂. *Biochemistry*, **40**, 4672–4678.
20. Stahelin, R. V., Long, F., Diraviyam, K., Bruzik, K. S., Murray, D. & Cho, W. (2002). Phosphatidylinositol 3-phosphate induces the membrane penetration of the FYVE domains of Vps27p and Hrs. *J. Biol. Chem.* **277**, 26379–26388.
21. Llopis, J., McCaffery, J. M., Miyawaki, A., Farquhar, M. G. & Tsien, R. Y. (1998). Measurement of cytosolic, mitochondrial, and Golgi pH in single living cells with green fluorescent proteins. *Proc. Natl Acad. Sci. USA*, **95**, 6803–6808.
22. Brett, C. L., Tukaye, D. N., Mukherjee, S. & Rao, R. (2005). The yeast endosomal Na⁺(K⁺)/H⁺ exchanger Nhx1 regulates cellular pH to control vesicle trafficking. *Mol. Biol. Cell*, **16**, 1396–1405.
23. Osborne, S. L., Thomas, C. L., Gschmeissner, S. & Schiavo, G. (2001). Nuclear PtdIns(4,5)P₂ assembles in a mitotically regulated particle involved in pre-mRNA splicing. *J. Cell Sci.* **114**, 2501–2511.
24. Lee, S. A., Eyeson, R., Cheever, M. L., Geng, J., Verkhusha, V. V., Burd, C. *et al.* (2005). Targeting of the FYVE domain to endosomal membranes is regulated by a histidine switch. *Proc. Natl Acad. Sci. USA*, **102**, 13052–13057.
25. van Paridon, P. A., de Kruijff, B., Ouwerkerk, R. & Wirtz, K. W. (1986). Polyphosphoinositides undergo charge neutralization in the physiological pH range: a ³¹P-NMR study. *Biochim. Biophys. Acta*, **877**, 216–219.
26. Hildebrand, J., Marique, D. & Vanhouche, J. (1975). Lipid composition of plasma membranes from human leukemic lymphocytes. *J. Lipid. Res.* **16**, 195–199.
27. Stahelin, R. V., Burian, A., Bruzik, K. S., Murray, D. & Cho, W. (2003). Membrane binding mechanisms of the PX domains of NADPH oxidase p40phox and p47phox. *J. Biol. Chem.* **278**, 14469–14479.
28. Kutateladze, T. G., Capelluto, D. G. S., Ferguson, C. G., Cheever, M. L., Kutateladze, A. G., Prestwich, G. D. & Overduin, M. (2004). Multivalent mechanism of membrane insertion by the FYVE domain. *J. Biol. Chem.* **279**, 3050–3057.
29. Marsh, D. (1996). Lateral pressure in membranes. *Biochim. Biophys. Acta*, **1286**, 183–223.
30. Gottlieb, R. A., Giesing, H. A., Zhu, J. Y., Engler, R. L. & Babior, B. M. (1995). Cell acidification in apoptosis: granulocyte colony-stimulating factor delays

- programmed cell death in neutrophils by up-regulating the vacuolar H(+)-ATPase. *Proc. Natl Acad. Sci. USA*, **92**, 5965–5968.
31. Moolenaar, W. H., Tsien, R. Y., van der Saag, P. T. & de Laat, S. W. (1983). Na⁺/H⁺ exchange and cytoplasmic pH in the action of growth factors in human fibroblasts. *Nature*, **304**, 645–648.
 32. Schuldiner, S. & Rozengurt, E. (1982). Na⁺/H⁺ antiport in Swiss 3T3 cells: mitogenic stimulation leads to cytoplasmic alkalinization. *Proc. Natl Acad. Sci. USA*, **79**, 7778–7782.
 33. Thangaraju, M., Sharma, K., Leber, B., Andrews, D.W., Shen, S. H. & Srikant, C. B. (1999). Regulation of acidification and apoptosis by SHP-1 and Bcl-2. *J. Biol. Chem.* **274**, 29549–29557.
 34. LaManna, J. C. (1996). Hypoxia/ischemia and the pH paradox. *Adv. Exp. Med. Biol.* **388**, 283–292.
 35. Punnia-Moorthy, A. (1987). Evaluation of pH changes in inflammation of the subcutaneous air pouch lining in the rat, induced by carrageenan, dextran and *Staphylococcus aureus*. *J. Oral. Pathol.* **16**, 36–44.
 36. Gerweck, L. E. & Seetharaman, K. (1996). Cellular pH gradient in tumor versus normal tissue: potential exploitation for the treatment of cancer. *Cancer Res.* **56**, 1194–1198.
 37. Myszka, D. G., Morton, T. A., Doyle, M. L. & Chaiken, I. M. (1997). Kinetic analysis of a protein antigen-antibody interaction limited by mass transport on an optical biosensor. *Biophys. Chem.* **64**, 127–137.